Iranian Journal of Basic Medical Sciences
ijbms.mums.ac.ir

Mechanistic pathways and *in silico* modeling of gallic acid–mediated protection against doxorubicin-induced nephrotoxicity in rats

Samet Tekin [1]*, Burak Çinar [2], Yusuf Dağ [1], Aslıhan Atasever [1], Merve Bolat [1], İsmail Bolat [1], Burak Batuhan Laçin [1], Emin Şengül [1], Serkan Yıldırım [1, 3], Mohamad Warda [1, 4]

[1] Atatürk University, Faculty of Veterinary Medicine, Department of Physiology, 25000 Erzurum, Turkey
[2] Atatürk University, Faculty of Medicine, Department of Medical Pharmacology, 25000 Erzurum, Turkey
[3] Kyrgyzstan-Turkey Manas University, Faculty of Veterinary Medicine, Department of Pathology, 720007 Bishkek, Kyrgyzstan
[4] Cairo University, Faculty of Veterinary Medicine, Department of Biochemistry, 3753450 Giza, Egypt

ARTICLE INFO

Article type:
Original

Article history:
Received: Aug 15, 2025
Accepted: Feb 1, 2026

Keywords:
Apoptosis
Doxorubicin
Gallic acid
Inflammation
Molecular docking
Nephrotoxicity
Oxidative stress

ABSTRACT

Objective(s): This study aimed to evaluate the protective effects of Gallic acid (GA) against (Doxorubicin) DOX-induced renal injury and to explore potential molecular interactions underlying its effects.

Materials and Methods: Fifty male rats were randomly assigned to five groups: Control, DOX, GA50+DOX, GA100+DOX, and GA100. DOX was administered as a single intraperitoneal dose on day 8 (40 mg/kg), while GA was given orally at 50 or 100 mg/kg for 10 consecutive days. Renal tissues were collected on day 11 and analyzed for oxidative stress markers, pro- and anti-inflammatory cytokines, and the apoptotic marker caspase-3 via ELISA. Immunohistochemistry assessed Nrf-2 and HO-1 expression, and histopathology evaluated structural alterations. Molecular docking simulations were performed for DOX/topoisomerase IIα (PDB ID: 4FM9) and GA/TNF-α (PDB ID: 2AZ5).

Results: GA significantly ameliorated DOX-induced oxidative stress, inflammatory cytokine imbalance, caspase-3 activation, and histological damage in a dose-dependent manner, while enhancing Nrf-2 and HO-1 expression. Docking analysis confirmed DOX binding to topoisomerase IIα and revealed strong GA–TNF-α binding affinity.

Conclusion: GA exerts substantial renoprotective effects against DOX-induced nephrotoxicity by modulating oxidative, inflammatory, and apoptotic pathways. The agreement between *in vivo* findings and *in silico* modeling supports GA as a potential complementary agent to reduce chemotherapy-related renal injury.

►Please cite this article as:
Tekin S, Çinar B, Dağ Y, Atasever A, Bolat M, Bolat İ, Laçin BB, Şengül E, Yıldırım S, Warda M. Mechanistic pathways and *in silico* modeling of gallic acid–mediated protection against doxorubicin-induced nephrotoxicity in rats. Iran J Basic Med Sci 2026; 29: 623-633. doi: https://dx.doi.org/10.22038/ijbms.2026.90473.19500

Introduction

Renal damage has emerged as a significant public health concern, with an increasing prevalence over time (1). Kidney diseases result from progressive damage to the nephrons. Damage to the kidneys can have multiple causes and may also occur as a side effect of drugs used to treat other diseases (2). Doxorubicin (DOX), an anthracycline group antibiotic, is used as an anticancer drug (3, 4) by suppressing DNA and RNA replication in tumor cells (5). Its clinical use is currently limited due to the serious organ damage and other side effects, including kidney diseases with accompanying proteinuria and hematuria complications (6, 7). Although the mechanism of acute cellular insult remains unclear, the primary contributor is the excessive production of reactive oxygen species (ROS) (8). DOX exposure induces the production of hydrogen peroxide, superoxide anions, and hydroxyl radicals in cells. Once metabolized by NADPH-cytochrome P-450, DOX is converted into a semiquinone free radical product that initiates the formation of superoxide anions and hydroxyl radicals with exaggeration of membrane lipid peroxidation (LPO) (9). Therefore, LPO serves as a critical marker of toxicity following doxorubicin (DOX) administration and is commonly assessed by measuring malondialdehyde (MDA) concentrations. In the rat model, DOX-induced nephrotoxicity is characterized by significant renal lipid peroxidation (10). Numerous studies have examined the oxidative damage induced by DOX, which leads to cellular oxidative stress and reduced endogenous anti-oxidants (11, 12). This imbalance triggers an immune response and inflammation (13), resulting in the overproduction of pro-inflammatory cytokines, including tumor necrosis factor-alpha (TNF-α), nitric oxide (NO), and cyclooxygenase-2 (COX-2). These factors contribute to the induction of apoptosis in renal nephrons (14, 15). DOX administration, therefore, induces oxidative stress, inflammation, and apoptosis, resulting in significant damage to renal nephrons.

*Corresponding author: Samet Tekin. Atatürk University, Faculty of Veterinary Medicine, Department of Physiology, 25000 Erzurum, Turkey Tel: +90 538 8347040, Fax: +90 442 2317113, Email: samet.tekin@atauni.edu.tr.

Given the multifaceted damage caused by DOX-induced oxidative stress and inflammation, it is crucial to explore potential therapeutic agents with anti-oxidant and anti-inflammatory properties to counteract these effects. Gallic acid (GA; 3,4,5-trihydroxybenzoic acid) and its derivatives are polyphenolic compounds found in grapes, mangoes, walnuts, and green tea. GA has demonstrated potent anti-oxidant, anticancer, antimicrobial, and anti-inflammatory activities across various experimental settings. Moreover, *in vivo* studies have revealed its efficacy in attenuating oxidative stress-induced damage (16).

This study aims to evaluate the protective effects of GA against DOX-induced nephrotoxicity by comprehensively analyzing oxidative stress markers, pro- and anti-inflammatory cytokines, apoptotic markers, and histopathological alterations. Additionally, molecular docking was employed to explore GA's potential interaction with TNF-α, providing mechanistic insight into its anti-inflammatory action.

Materials and Methods

Chemicals

Doxorubicin (commercial injectable formulation) was obtained from Koçak Farma (Istanbul, Türkiye). Gallic Acid (≥99%, CAS No: 149-91-7) was purchased from Sigma-Aldrich (St. Louis, MO, USA). ELISA kits were provided by BT Lab (Shanghai, China).

Animals and experimental design

The study was approved by Atatürk University Experimental Animals Local Ethics Committee (HADYEK Decision No: 2024/111). Sprague Dawley rats used in this study were obtained from Atatürk University Medical Experimental Research and Application Centre (ATADEM). A total of 50 male rats with an average weight between 200 and 250 g were included. The rats were maintained in an environment at 25 °C, 60 ± 10% humidity, and a 12 hr light/dark cycle. Access to both water and pellet feed was provided as required.

Each experimental group consisted of 10 Sprague-Dawley rats (n = 10). A formal a priori power analysis could not be performed because variance estimates for multiple biochemical, histopathological, and immunofluorescence endpoints were unavailable prior to the study. However, a group size of n = 10 rats is widely accepted in doxorubicin-induced nephrotoxicity models and is considered sufficient to detect biologically meaningful differences across multi-parameter oxidative, inflammatory, and apoptotic markers. This sample size also aligns with previously published toxicology studies using similar methodologies and endpoints. Therefore, we adopted n = 10 per group, consistent with the established literature. The nephrotoxicity model was validated based on established literature demonstrating that a single intraperitoneal dose of DOX (40 mg/kg) reliably induces renal injury in rats (17). The DOX dose (40 mg/kg, single IP on day 8) was selected based on previously validated acute nephrotoxicity models, which used the same regimen to reliably induce oxidative, inflammatory, and apoptotic renal injury. All animals tolerated this dose without unexpected mortality, consistent with prior studies (17-19).

Before starting the experiment, all rats were weighed and divided into the following five groups:

Group I (Control): Rats received 1 ml of ddH_2O via intragastric (i.g.) administration for 10 days.

Group II (DOX): Rats received 1 ml of ddH_2O i.g. for 10 days, with a single intraperitoneal (IP) dose of DOX (40 mg/kg) on the 8th day (17).

Group III (GA50+DOX): Rats were administered GA at 50 mg/kg i.g. for 10 days, with a single IP dose of DOX (40 mg/kg) on the 8th day (17, 20).

Group IV (GA100+DOX): Rats received GA at 100 mg/kg i.g. for 10 days, along with a single IP dose of DOX (40 mg/kg) on the 8th day (17, 20).

Group V (GA100): Rats were given GA at 100 mg/kg i.g. for 10 days (20).

No mortality was observed throughout the experimental period, and all animals completed the study. At the end of the experiments, animals were weighed before intracardiac blood samples were collected under sevoflurane anesthesia. After cervical dislocation, the kidneys were excised and weighed. After saline washing, a portion of the kidney tissue was immediately fixed in formaldehyde for histopathological, immunohistochemical, and immunofluorescence examinations, while the remaining tissue was promptly frozen in liquid nitrogen and stored at -80 **°C** until biochemical analyses.

Randomization and blinding

All animals were randomly assigned to experimental groups using a computer-generated randomization list to minimize allocation bias. During tissue processing, histopathological scoring, and immunofluorescence evaluation, the investigator performing the analyses was fully blinded to group assignments. Biochemical assays (ELISA) were performed using coded samples to ensure unbiased quantification.

Homogenization of kidney tissue

Kidney tissue samples were equally weighed and transferred to screw cap tubes. A total volume of 1500 µl of phosphate-buffered saline (PBS) solution was added, and tissue lysis was performed using a Magna Lyser homogenizer. The homogenates were then centrifuged at 5000 rpm for 10 min at 4 °C. The recovered supernatants were carefully collected and transferred to clean Eppendorf tubes (21).

Biochemical analyses

Analysis of oxidant parameters and anti-oxidant enzymes

The ELISA Study was conducted according to the procedures specified in the purchased commercial kits. The ELISA Plate Reader (Bio-Tek, Winooski, VT, USA) was configured to read at 450 nm wavelength. Then, measurements of malondialdehyde (MDA), glutathione (GSH), superoxide dismutase (SOD), and catalase (CAT) oxidant enzyme parameters in the supernatants were performed according to the ELISA kit protocols (21).

Analysis of inflammation markers

Interleukin-1 beta (IL-1β), interleukin-4 (IL-4), interleukin-6 (IL-6), tumor necrosis factor alpha (TNFα), interleukin-10 (IL-10), nuclear factor kappa-B (NF-κB), cyclooxygenase-1 (COX-1) and inducible nitric oxide synthase (iNOS) in the supernatants, Cyclooxygenase-2 (COX-2), Peroxisome proliferator-activated receptor (PPAR), Interferon-γ (IFN-γ) and parameter measurements were performed following the instructions provided in the

protocols of ELISA kits. Further assessment of apoptosis was performed by measuring caspase-3 (CAS-3) levels in the tissue supernatants using ELISA, according to the manufacturer's protocol (21).

Histopathological examination

Tissue samples were fixed in 10% formaldehyde solution for 48 hr and embedded in paraffin blocks after routine tissue follow-up procedures. Four µm-thick sections were cut from each block, and the preparations were subjected to histopathological examination, stained with hematoxylin-eosin (HE), and examined by light microscopy (Olympus BX51, Japan). The sections were evaluated as absent (-), mild (+), moderate (++), and severe (+++) according to histopathological features (22).

Double immunofluorescence examination

For immunoperoxidase examination, tissue sections taken on adhesive (Poly-L-lysine) slides were deparaffinized and dehydrated. Then, endogenous peroxidase was inactivated in 3% H_2O_2 for 10 min. The tissues were then boiled in 1% antigen retrieval solution (citrate buffer (pH+6.1) 100X) and allowed to cool at room temperature. The sections were incubated with a protein block for 5 min to prevent nonspecific background staining in the tissues. Then, primary antibody (Nrf2; Cat. No.: ab89443; Reconstitution Ratio: 1/100; US) was applied to the tissues and incubated according to the instructions for use. Immunofluorescence secondary antibody (FITC; Cat. No. ab6785; dilution 1/1000) was used as the secondary marker and incubated in the dark for 45 min. Then, the second primary antibody (HO-1, Cat. No.: ab189491, Dilution Ratio: 1/100, US) was applied to the tissues and incubated according to the instructions for use. Immunofluorescence secondary antibody (Texas Red; Cat. No. ab6719; dilution 1/1000 in the UK) was used as the secondary marker and incubated in the dark for 45 min. DAPI in mounting medium (Cat. No: D1306; Reconstitution Ratio: 1:200, UK) was applied to the tissue sections, which were then incubated in the dark for 5 min. Coverslips were carefully placed over the sections, and the stained slides were examined using a fluorescence microscope equipped with a Zeiss AXIO attachment (Germany) (23).

Molecular docking and MM-GBSA analysis of gallic acid/TNF-α and doxorubicin/topoisomerase II-α interactions

In silico molecular docking and binding free energy analyses were conducted using Schrödinger Maestro (licensed version 2025/1). Molecular docking was used to evaluate the interaction of Dox with the active site of human topoisomerase II-α (Top2-α; PDB ID: 4FM9), a site previously characterized for its binding with inhibitors such as Methoxantrone and Amsacrine (24). The docking grid was set to 20×20×20 Å, centered on the active site where the ligands are located. To further assess the potential protective mechanism of GA against Doxorubicin-induced DNA damage and nephrotoxicity, molecular docking and MM-GBSA (Molecular Mechanics Generalized Born Surface Area) binding energy calculations were also performed targeting the tumor necrosis factor-alpha (TNF-α) receptor (PDB ID: 2AZ5), based on the binding site described by Wendorff et al. (2012) (25).

TNF-α was selected as a docking target because it plays a central role in DOX-induced inflammatory responses in renal tissue. DOX is known to activate NF-κB–mediated cytokine release, leading to increased TNF-α expression, which contributes to tubular injury, oxidative stress, and apoptosis in kidney cells. Therefore, evaluating the interaction between GA and TNF-α provides mechanistic insight into the potential anti-inflammatory effects of GA.

Topoisomerase IIα (Top2α) was chosen as the target for DOX because its DNA-binding inhibition is the primary mechanism through which DOX exerts cytotoxic effects. Top2α poisoning leads to DNA strand breaks, mitochondrial dysfunction, and subsequent apoptotic signaling events also implicated in DOX-induced nephrotoxicity. Docking DOX with Top2α thus verifies the expected binding profile of DOX and validates the computational approach used in the study.

Statistical analysis

All statistical analyses were performed using GraphPad Prism 10. Data were first evaluated for normality using the Shapiro–Wilk test and for homogeneity of variances using Levene's test. Variables that met both assumptions were analyzed using one-way ANOVA followed by Tukey's *post hoc* test. For parameters that did not satisfy normality or homogeneity, non-parametric tests were applied, including the Kruskal–Wallis test followed by Dunn's *post hoc* test or the Mann–Whitney U test for pairwise comparisons. All biochemical and immunoassay data are presented as mean ± SD, whereas histopathological scores are expressed as median (IQR). A P-value<0.05 was considered statistically significant.

Results

Effects of doxorubicin and gallic acid on live and kidney weights of rats

When the initial body weights, final body weights, and kidney weights obtained in the DOX-induced kidney injury model were evaluated, no statistically significant differences were observed between groups (P>0.05; Table 1).

Effects of doxorubicin and gallic acid on MDA and GSH levels and SOD, GPx, and CAT activities

Doxorubicin administration markedly disrupted the oxidative stress profile. Accordingly, MDA levels were significantly higher in the DOX group than in the control group (P<0.001). GA50+DOX treatment reduced MDA levels relative to the DOX group (P<0.001), whereas

Table 1. Effects of doxorubicin (DOX) and gallic acid (GA) on initial and final body weights, as well as kidney weights, of rats in the experimental groups

Parameters	Control	DOX	GA50+DOX	GA100+DOX	GA100
Initial Live Weight (g)	277±14,9[a]	272±15,99[a]	276±17,85[a]	277±13,46[a]	277±9,93[a]
Final Live Weight (g)	295±22,4[a]	288±16,60[a]	289±8,8[a]	286±19,40[a]	301±14,27[a]
Kidney Weights (g)	1,16 ± 0,09[a]	0,98 ± 0,13[a]	1,02 ± 0,13[a]	1,04 ± 0,09[a]	1,08 ± 0,21[a]

Values are expressed as mean ± SD. Different superscript letters in the same row indicate statistically significant differences between groups (P< 0.05).

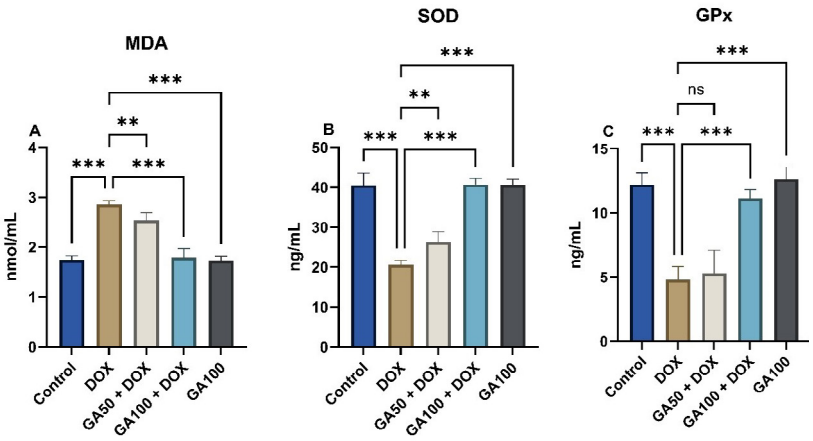

Figure 1. Effects of DOX and GA administration on MDA (A), SOD (B), and GPx (C) levels in the rat experimental groups
Significant differences between groups are denoted by *P<0.05, **P<0.01, ***P<0.001; n = 10.
DOX: Doxorubicin; GA: Gallic acid; MDA: Malondialdehyde; SOD: Superoxide dismutase; GPx: Glutathione peroxidase

GA100+DOX produced an even more pronounced reduction, bringing MDA levels close to those of the control (P<0.001). The GA100 group exhibited MDA concentrations comparable to the control (P>0.05, Figure 1).

Analysis of anti-oxidant enzyme activities revealed that SOD and GPx levels were significantly reduced in the DOX group (P<0.001). GA50+DOX treatment produced a moderate improvement in both enzymes compared with the DOX group (for SOD, P<0.001; for *GPx*, P<0.01). In contrast, GA100+DOX elicited a markedly stronger anti-oxidant response, restoring SOD and GPx activities to levels close to those of the control group (P<0.001). GA100 alone did not produce a significant change in either enzyme (P>0.05, Figure 1).

DOX administration markedly reduced GSH and CAT levels in kidney tissue (P<0.001). In the GA50+DOX group, GSH levels showed a significant increase compared with the DOX group (P<0.001), whereas the improvement in CAT levels was more limited (P<0.01). The most pronounced recovery was observed in the GA100+DOX group; both parameters increased significantly relative to DOX (P<0.001) and reached levels comparable to the control group (P>0.05, Figure 2).

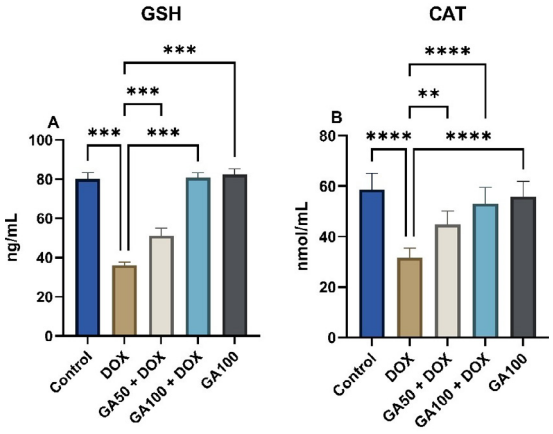

Figure 2. Effects of DOX and GA administration on GSH (A) and CAT (B) levels in the rat experimental groups
Significant differences between groups are denoted by *P<0.05, **P<0.01, ***P<0.001; n = 10.
DOX: Doxorubicin; GA: Gallic acid; GSH: Glutathione

Effects of gallic acid on doxorubicin-induced nephrotic inflammation

DOX administration elicited a pronounced pro-inflammatory response in kidney tissue, significantly increasing both TNF-α and IL-1β levels (P<0.001). Although GA50+DOX treatment reduced TNF-α (P<0.01) and IL-1β (P<0.01) levels compared with the DOX group, these parameters did not fully return to control values. In contrast, GA100+DOX produced the most robust improvement, lowering both TNF-α and IL-1β to P<0.001 relative to DOX and approaching control levels (Figure 3).

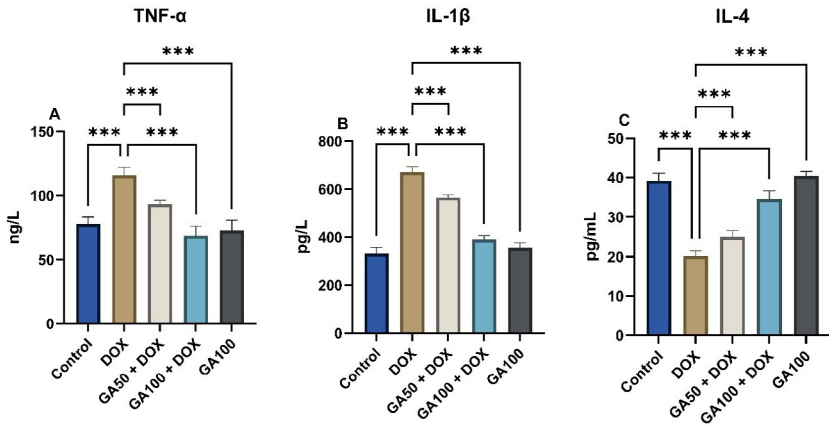

Figure 3. Effects of DOX and GA administration on TNF-α (A), IL-1β (B), and IL-4 (C) levels in the rat experimental groups
Significant differences between groups are denoted by *P<0.05, **P<0.01, ***P<0.001; n = 10.
DOX: Doxorubicin; GA: Gallic acid; TNF-α: Tumor necrosis factor-alpha

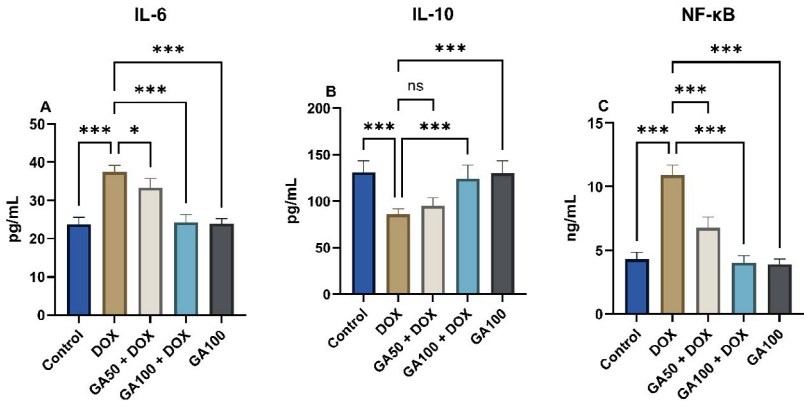

Figure 4. Effects of DOX and GA administration on IL-6 (A), IL-10 (B), and NF-κB (C) levels in the rat experimental groups
Significant differences between groups are denoted by *P<0.05, **P<0.01, ***P<0.001; n=10.
DOX: Doxorubicin; GA: Gallic acid; IL-10: Interleukin-10; NF-κB: Nuclear factor kappa-B

DOX administration also caused a marked decrease in IL-4, an anti-inflammatory marker (P<0.001). GA50+DOX treatment resulted in a significant improvement in IL-4 levels compared with DOX (P<0.01), but the greatest recovery was observed in the GA100+DOX group, in which IL-4 levels increased to P<0.001 relative to DOX and approached control levels (Figure 3).

DOX administration induced a pronounced inflammatory response in kidney tissue, resulting in a significant increase in IL-6 and NF-κB levels (P<0.001). GA50+DOX treatment produced improvement in both parameters compared with the DOX group, with IL-6 showing a P<0.05 reduction and NF-κB showing a P<0.001 reduction. The most substantial improvement was observed in the GA100+DOX group, in which both IL-6 and NF-κB levels decreased to P<0.001 relative to DOX and approached control levels (Figure 4).

Conversely, IL-10, an anti-inflammatory marker, was significantly reduced following DOX administration (P<0.001). GA50+DOX treatment did not produce a meaningful increase in IL-10 levels compared with the DOX group (P>0.05). In contrast, GA100+DOX administration markedly increased IL-10 levels relative to the DOX group (P<0.001) (Figure 4).

Effects of gallic acid on eNOS and COX-2 levels in doxorubicin-induced nephrotoxicity

DOX administration significantly reduced eNOS levels in kidney tissue (P<0.001). Although the GA50+DOX group showed an increase in eNOS levels compared with the DOX group, values remained markedly lower than those of the control (P<0.001). The greatest improvement was observed in the GA100+DOX group, where eNOS levels increased significantly relative to the DOX group (P<0.001) and approached those of the control (Figure 5).

In contrast, COX-2 levels were markedly elevated following DOX administration (P<0.001). Although GA50+DOX treatment produced a partial reduction in COX-2 levels, this change was not statistically significant compared with the DOX group (P>0.05). GA100+DOX treatment, however, significantly decreased COX-2 levels relative to the DOX group (P<0.001) (Figure 5).

Effects of gallic acid on IFN-γ and PPAR-γ levels in doxorubicin-induced nephrotoxicity

DOX administration elicited a marked pro-inflammatory response in kidney tissue, resulting in a significant increase

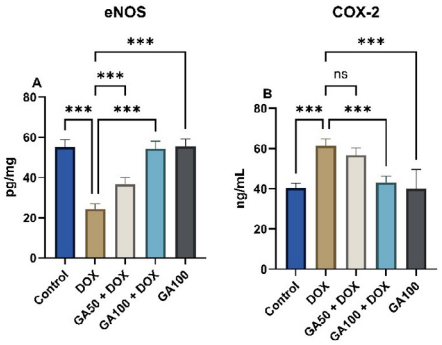

Figure 5. Effects of DOX and GA administration on eNOS (A) and COX-2 (B) levels in the rat experimental groups
Significant differences between groups are denoted by *P<0.05, **P<0.01, ***P<0.001; n=10.
DOX: Doxorubicin; GA: Gallic acid; eNOS: Endothelial NOS; COX-2: Cyclooxygyenase-2

in IFN-γ levels compared with the control group (P<0.001). IFN-γ levels in the GA50+DOX group were lower than those in the DOX group, with a statistically significant difference between the two (P<0.001). The most pronounced improvement was observed in the GA100+DOX group, in which IFN-γ levels were significantly lower than in the DOX group (P<0.001) and approached control levels (Figure 6).

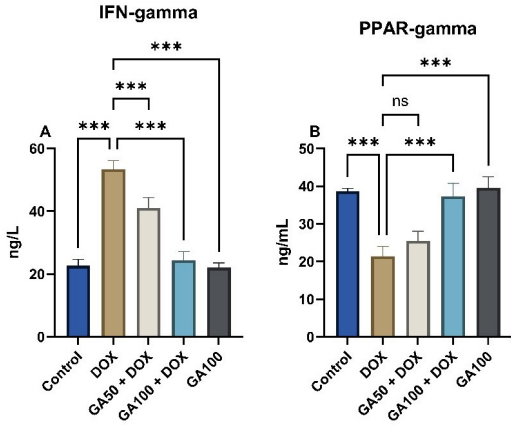

Figure 6. Effects of DOX and GA administration on IFN-γ (A) and PPAR-γ (B) levels in the rat experimental groups
Significant differences between groups are denoted by *P<0.05, **P<0.01, ***P<0.001; n=10.
DOX: Doxorubicin; GA: Gallic acid; IFN-γ: Interferon-γ; PPAR-γ: Proliferator-activated receptor

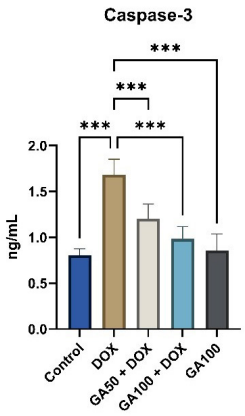

Figure 7. Effects of DOX and GA administration on CASP3 level in the rat experimental groups
Significant differences between groups are denoted by *P<0.05, **P<0.01, ***P<0.001; n=10. DOX: Doxorubicin; GA: Gallic acid

In contrast, PPAR-γ levels were markedly suppressed in the DOX-treated group (P<0.001). Although the GA50+DOX group showed a slight increase in PPAR-γ levels compared with the DOX group, this difference was not statistically significant (P>0.05). GA100+DOX treatment significantly increased PPAR-γ levels relative to the DOX group (P<0.001) (Figure 6).

Effects of gallic acid on CASP3 levels in doxorubicin-induced nephrotoxicity

DOX administration induced marked apoptotic activation in kidney tissue, and CASP3 levels increased significantly compared with the control group (P<0.001). Although GA50+DOX treatment produced a significant reduction in CASP3 levels relative to the DOX group (P<0.01), the values remained higher than those of the control group. The most pronounced improvement was observed in the GA100+DOX group, in which CASP3 levels were significantly reduced compared with the DOX group (P<0.001) and approached control levels (Figure 7).

Histopathological findings

Histopathological examination of kidney tissues from the control group revealed a normal histological appearance (Figure 8). In contrast, the DOX-treated group showed severe degeneration and necrosis of the tubular epithelium, along with marked hyperemia in the glomerular and interstitial spaces (Figure 8). In the GA50+DOX group, moderate degeneration, mild necrosis in the tubular epithelium, and vascular hyperemia were observed. Kidney tissues from the GA100+DOX group exhibited only mild degeneration of the tubular epithelium and vascular hyperemia. Compared with the DOX group, GA100+DOX markedly reduced tubular degeneration, necrosis, and vascular hyperemia. Meanwhile, the GA100 group exhibited normal histological architecture, comparable to that of the control group (Figure 8).

Immunofluorescence findings

Immunofluorescence analysis of kidney tissues from the control group revealed mild cytoplasmic expression of Nrf-2 and HO-1 in the tubular epithelium (Figure 9). In the

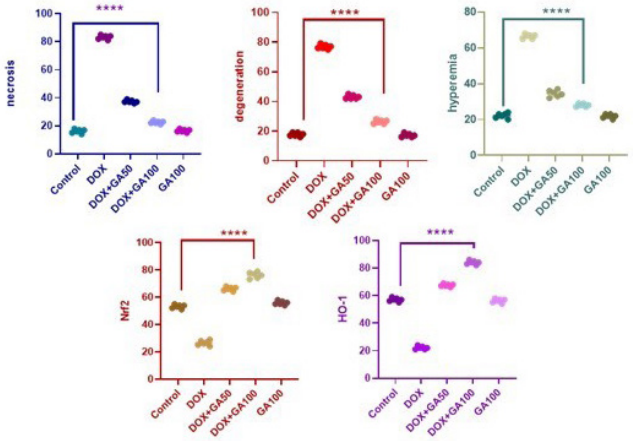

Figure 9. Statistical analysis of histopathological findings and immunofluorescence staining results in rat kidney tissue
Significant differences were observed in tubule epithelial degeneration (****P<0.0001), tubule epithelial necrosis (****P<0.0001), hyperemia (****P<0.0001), Nrf-2 expression levels (****P<0.0001), and HO-1 expression levels (****P<0.0001). The Mann-Whitney U test was used to analyze histopathological data, whereas one-way ANOVA followed by Tukey's test was used to analyze immunofluorescence data. Nrf-2: Nuclear factor erythroid 2-related factor 2; HO-1: Heme oxygenase-1

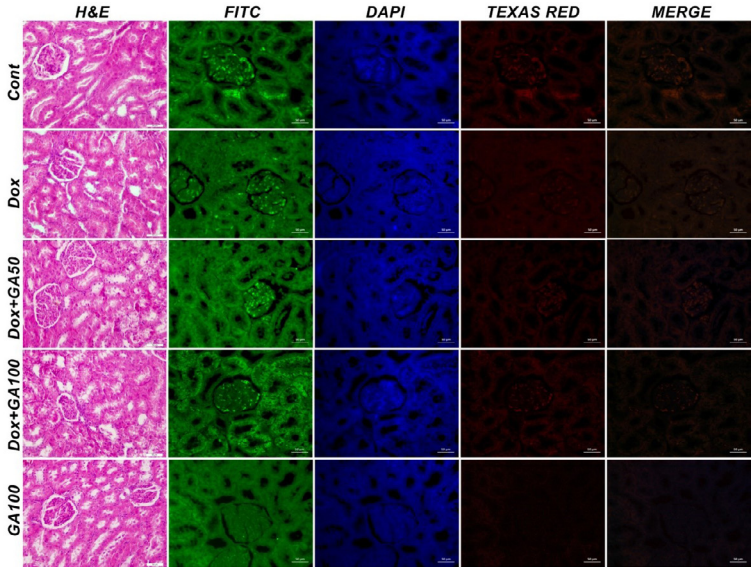

Figure 8. Histological examination of kidney tissue showing degenerative and necrotic changes in the rat tubules (H&E, Bar: 50 µm)
Immunofluorescence images displaying intracytoplasmic Nrf-2 expression (FITC) and HO-1 expression (Texas Red) in renal tubular epithelium (IF, Bar: 50 µm). H&E: Hematoxylin and eosin; Nrf-2: Nuclear factor erythroid 2-related factor 2; HO-1: Heme oxygenase-1; IF: Immunofluorescence; DOX: Doxorubicin; GA: Gallic acid

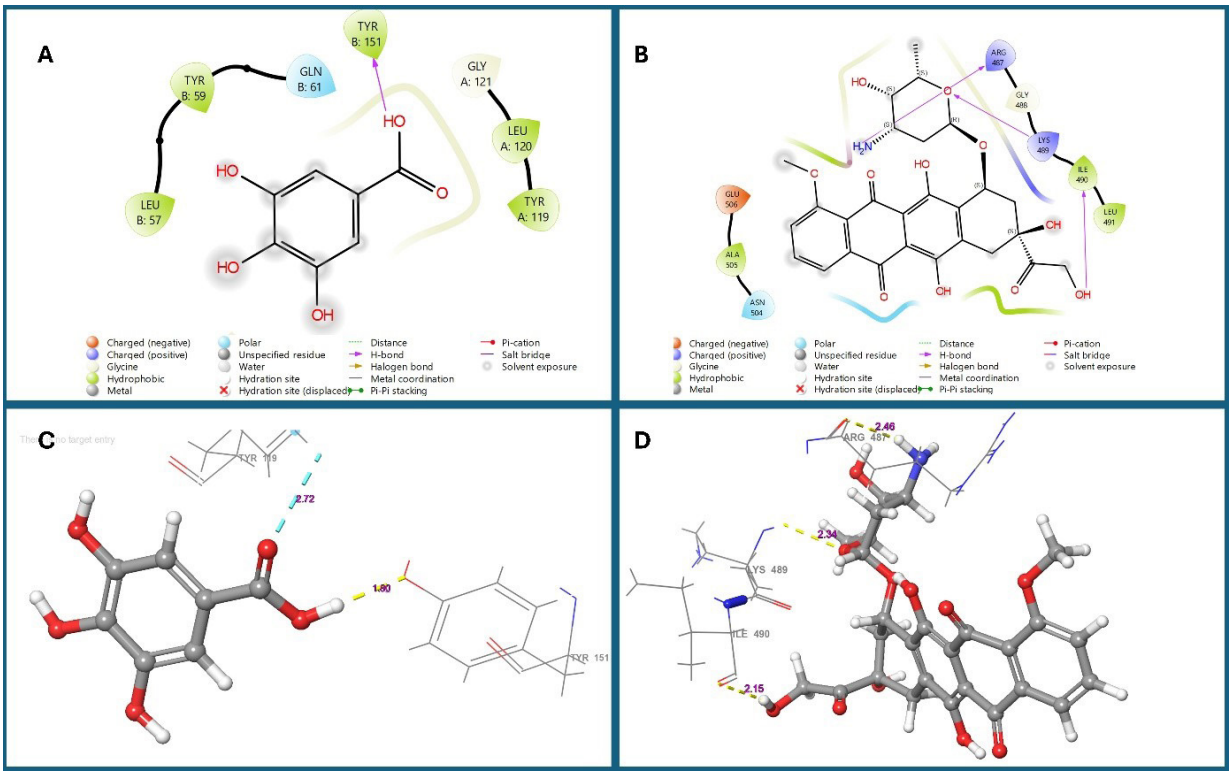

Figure 10. *In silico* molecular docking interactions of gallic acid and doxorubicin with TNF-α and topoisomerase II-α (a, c) Gallic acid; (b, d) Doxorubicin TNF-α: Tumor necrosis factor-alpha

DOX-treated group, very mild Nrf-2 and HO-1 expression was detected in the cytoplasm of tubular epithelial cells. In the GA50+DOX group, moderate cytoplasmic expression of both Nrf-2 and HO-1 was found. Kidney tissues from the GA100+DOX group showed strong Nrf-2 and HO-1 expression in the tubular epithelium. Relative to DOX-treated kidneys, GA100+DOX produced a marked increase in Nrf-2 and HO-1 expression. In contrast, the GA100 group displayed mild expression levels, similar to the control (Figure 9). Scoring and statistical analyses of these histopathological and immunofluorescence findings are summarized in Figure 9.

Molecular docking and MMGBSA analysis results

The docking poses of gallic acid with TNF-α and DOX with topoisomerase IIα are shown in Figure 10. Docking scores and Glide energies for both ligands are presented in Table 2. Gallic acid showed a docking score of −5.105 and a Glide energy of −31.762 kcal/mol for TNF-α, whereas DOX showed a docking score of −3.908 and a Glide energy of −52.255 kcal/mol for topoisomerase IIα (Table 2).

Table 2. Molecular Docking Scores of Gallic Acid/TNF alpha and Doxorubicin/ topoisomerase II alpha

Docking scores	Docking score	Glide energy
Gallic Acid	-5.105	-31.762
Doxorubicin	-3.908	-52.255

Key hydrogen-bond interactions and distances between gallic acid or DOX and their respective target residues are summarized in Table 3. Gallic acid formed an aromatic hydrogen bond with TYR119 (2.72 Å) and a hydrogen bond with TYR151 (1.80 Å) of TNF-α. DOX formed hydrogen bonds with ARG487 (2.46 Å), LYS489 (2.34 Å), and ILE490 (2.15 Å) of topoisomerase IIα.

The MM-GBSA binding free-energy components for gallic acid and DOX are listed in Table 4. The total ΔG_bind values were −23.53 kcal/mol for gallic acid and −29.13 kcal/mol for doxorubicin. Coulombic and van der Waals

Table 3. Molecular docking analysis: Distances between ligand-binding amino acids and atoms for Gallic acid/TNF-alpha and Doxorubicin/topoisomerase II alpha

Docking complex	Bond + amino acid	Atom1 (Receptor)	Atom2 (Ligand)	Distance (Angstrom= Å)
Gallic Acid	Aromatic H Bond with TYR119	H:3882	O:4296	2.72
	Hydrogen Bond with TYR 151	O:2055	H:4309	1.80
	Hydrogen Bond with ARG 487	O:396	H:11954	2.46
	Hydrogen Bond with LYS 489	H:6318	O:11900	2.34
Doxorubicin	Hydrogen Bond with ILE 490	O:420	H:11961	2.15

Table 4. Molecular docking analysis results for Gallic Acid and Doxorubicin: Binding energy components in kcal/mol

Title	Gallic acid	Doxorubicin
r_psp_MMGBSA_dG_Bind	-23.534380992470687	-29.126819722201617
r_psp_MMGBSA_dG_Bind_Coulomb	-13.302442397663981	-19.064396898458654
r_psp_MMGBSA_dG_Bind_Covalent	0.642500777580608	1.4262080180405974
r_psp_MMGBSA_dG_Bind_Hbond	-0.6235093048276497	-1.548388406184074
r_psp_MMGBSA_dG_Bind_Lipo	-5.244273707241518	-7.437939144430402
r_psp_MMGBSA_dG_Bind_Packing	-0.06073424076777911	-1.7568465997739224
r_psp_MMGBSA_dG_Bind_SelfCont	0.0	0.0
r_psp_MMGBSA_dG_Bind_Solv_GB	13.004568183315314	30.12164459788073
r_psp_MMGBSA_dG_Bind_Solv_SA		
r_psp_MMGBSA_dG_Bind_vdW	-17.95049030286259	-30.86710128927689

contributions, as well as solvation components, are also shown in Table 4.

Discussion

The kidneys are highly susceptible to chemotherapeutic injury owing to their central roles in filtration, xenobiotic handling, and metabolic regulation. Among anticancer agents, DOX is well known to induce oxidative, inflammatory, and apoptotic disturbances that compromise renal integrity (26). In this study, we evaluated the nephrotoxic impact of DOX and demonstrated that gallic acid (GA), a phenolic compound with established anti-oxidant activity, provides significant protection against DOX-induced renal injury.

DOX is widely documented to induce nephrotoxicity through excessive ROS generation, lipid peroxidation, and inflammatory activation, ultimately leading to tubular degeneration and glomerular dysfunction (27, 28). In accordance with these mechanistic insights, DOX administration in our study markedly elevated MDA levels while suppressing key anti-oxidant defenses (SOD, GPx, CAT, and GSH), indicating a pronounced oxidative imbalance in renal tissue.

GA significantly reversed these oxidative alterations by enhancing endogenous anti-oxidant enzyme activities and reducing lipid peroxidation. Similar renoprotective effects of GA against chemically induced kidney injury have been reported in recent studies, which demonstrate its robust free radical–scavenging capacity (29-31). DOX also triggered a strong pro-inflammatory response, as reflected by increased NF-κB–related cytokines (TNF-α, IL-1β, IL-6), consistent with previously reported inflammatory cascades in DOX-induced renal injury (32-34). GA supplementation attenuated these pro-inflammatory mediators and restored IL-4 and IL-10 levels, suggesting a shift toward an anti-inflammatory milieu in the kidney.

Nitric oxide (NO) plays an important role in renal hemodynamics and tubular homeostasis (35). Among the nitric oxide synthase isoforms, endothelial NOS (eNOS) generates NO under physiological conditions and contributes to anti-oxidant defense and cytoprotection, whereas inducible NOS (iNOS) is activated under pathological stress and promotes oxidative injury and apoptosis (35, 36). In our study, DOX administration markedly suppressed eNOS levels, while GA treatment restored eNOS expression, suggesting a protective endothelial response consistent with previous observations that phenolic compounds can enhance eNOS activity.

In addition, recent studies have shown that DOX stimulates inflammatory pathways by inducing the production of pro-inflammatory mediators, such as COX-2 (37). Up-regulation and overexpression of COX-2 are mainly associated with inflammation, uncontrolled cell proliferation, growth, metastasis, neovascularization, and angiogenesis that eventually lead to cancer (38). One study showed that administration of DOX significantly increased COX-2 levels (19). In our study, DOX administration increased this level, as observed in other studies, whereas GA administration brought it closer to the control level.

Macrophages residing in the kidney play essential roles in renal homeostasis and injury responses, with pro-inflammatory M1 macrophages contributing to tissue damage and M2 macrophages supporting repair. Experimental models have demonstrated that impairment of PPAR-γ signaling in macrophages enhances renal inflammation and exacerbates tissue injury (39, 40). Conversely, activation of PPAR-γ has been shown to shift macrophage polarization toward a reparative phenotype and attenuate inflammatory signaling in renal disease models (41). Consistent with these findings, GA has been reported to modulate inflammatory pathways through mechanisms involving PPAR-γ activation and redox regulation (42, 43).

Interferon-γ (IFN-γ) is a potent pro-inflammatory cytokine that contributes to renal injury by amplifying immune activation and disrupting mesangial cell function (44). Recent studies indicate that GA can suppress IFN-γ-producing immune cells, thereby exerting anti-inflammatory effects (45). In agreement with these observations, the present study demonstrated that GA markedly reduced renal IFN-γ levels while enhancing PPAR-γ activity, suggesting a protective immunomodulatory profile.

Caspase-3 is a central executioner of apoptosis, and its activation is strongly associated with DOX-induced mitochondrial injury in renal tubular cells (46, 47). Consistent with reported findings, DOX markedly increased caspase-3 activation in our study, whereas GA administration significantly attenuated this apoptotic

response. Previous research also supports the anti-apoptotic properties of GA across various tissues (48), consistent with our results.

Upon histopathological evaluation of the results obtained in our study, severe degeneration, necrosis, and hyperemia were observed in the renal tissues of DOX-treated rats, particularly in the glomerular and interstitial spaces. This observation aligns with a previous study in which histopathological examination revealed tubulointerstitial and glomerular damage in the kidneys of DOX-treated rats (19). In our study, the use of GA100 in combination with DOX significantly reduced degeneration, necrosis, and hyperemia.

The Nrf-2/HO-1 pathway is a key player in the assessment of oxidative stress (49). Nrf-2, a transcription factor, regulates cellular redox balance and anti-oxidant responses, particularly in phase II detoxification reactions (50). Under normal conditions, Nrf-2 is predominantly in the cytoplasm, but upon ROS accumulation, it dissociates from Keap-1, translocates to the nucleus, and activates protective genes (51). If Nrf-2 levels are insufficient, mitochondrial damage and apoptosis are inevitable (52). Thus, increasing Nrf-2 activation could serve as an effective therapeutic strategy (53). By enhancing Nrf-2 levels, anti-oxidant defense systems like HO-1 and NQO-1 are activated, significantly reducing oxidative stress (54). Consistent with our findings, a previous study reported low Nrf-2 and HO-1 levels in kidney tissues of DOX-treated rats (55). In contrast, we found that GA administration effectively increased Nrf-2 and HO-1 levels, thereby suppressing oxidative stress.

Molecular docking analyses were performed to explore potential molecular interactions relevant to DOX-induced nephrotoxicity. DOX demonstrated strong binding affinity toward topoisomerase II-α (Top2α), consistent with previous reports identifying Top2α-mediated DNA damage and apoptotic signaling as central mechanisms of DOX-induced renal injury (56). In contrast, GA exhibited a moderate binding interaction with TNF-α. Importantly, this predicted interaction should not be interpreted as a direct mechanism for reducing TNF-α production. As highlighted in recent mechanistic studies, DOX-induced nephrotoxicity is strongly driven by activation of NF-κB–dependent inflammatory pathways, which subsequently elevate TNF-α levels (56, 57). Therefore, the *in vivo* decrease in TNF-α observed in GA-treated groups is more plausibly explained by upstream inhibition of NF-κB signaling, rather than direct interference with TNF-α protein structure. Furthermore, independent anti-inflammatory studies demonstrate that GA modulates cytokine expression primarily through PPAR-γ activation and redox regulation rather than direct receptor binding (43). This supports the interpretation that docking provides supplementary insight into potential molecular contacts but does not account for the transcriptional down-regulation observed *in vivo*. These revisions clarify that the docking results complement, rather than mechanistically explain, the ELISA findings, thereby addressing the reviewer's concern.

This study has several limitations that should be acknowledged. First, only male rats were used, which may limit the generalizability of the findings to both sexes, given the known sex-dependent variability in renal responses to oxidative stress and chemotherapeutic injury. Second, the study focused on acute nephrotoxicity and did not include long-term follow-up to evaluate chronic renal alterations or recovery patterns after treatment cessation. Third, although key inflammatory, oxidative, and apoptotic markers were analyzed, additional molecular assays, such as Western blotting or gene-expression profiling, would provide stronger mechanistic validation, particularly for pathways inferred from in silico analyses. Finally, the doses of gallic acid were selected based on previously published toxicological studies; however, future research should incorporate dose–response modeling and pharmacokinetic evaluation to better define optimal therapeutic ranges. These limitations should be considered when interpreting the findings.

Conclusion

Gallic acid provided significant protection against doxorubicin-induced nephrotoxicity by attenuating oxidative stress, normalizing inflammatory cytokine profiles, suppressing apoptosis, and activating the Nrf2/HO-1 anti-oxidant pathway. The biochemical, molecular, and histopathological findings consistently demonstrated a dose-dependent renoprotective effect. Molecular docking supported these observations by revealing strong GA–TNF-α interactions, suggesting direct modulation of inflammatory signaling. Collectively, these findings indicate that gallic acid represents a promising adjunctive therapeutic candidate for reducing chemotherapy-related renal injury.

Acknowledgment

This study did not receive any specific grant from funding agencies in the public, commercial, or not-for-profit sectors.

Availability of Data and Materials

The datasets used and/or analyzed during the current study are available from the corresponding author upon reasonable request.

Ethical approval

This study protocol was approved by the Atatürk University Animal Experiments Local Ethics Committee (HADYEK, Decision No: 2024/111).

Authors' Contributions

The study's conception and design involved the active participation of all authors. S T, E Ş, S Y, B Ç, Y D, A A, M B, İ B, BB L, M W, and A H prepared materials, collected data, and conducted analyses. S Y performed pathology studies. B C conducted *in silico* studies. S T, M W, and A H skillfully crafted both the initial draft and the final, scientifically refined version of the manuscript. The manuscript underwent critical review and refinement in subsequent iterations, with valuable input from all authors. The final version of the manuscript was thoroughly reviewed and unanimously approved by all authors.

Conflicts of Interest

The authors declare that they have no conflicts of interest with anyone concerning this article.

Declaration

The authors declare that the article, tables, and figures were not written/ created by AI and AI-assisted Technologies.

References

1. Hrenak J, Arendasova K, Rajkovicova R, Aziriova S, Repova K, Krajcirovicova K, *et al.* Protective effect of captopril, olmesartan, melatonin and compound 21 on doxorubicin-induced nephrotoxicity in rats. Physiol Res 2013; 62: S181-189.
2. Petho AG, Tapolyai M, Csongradi E, Orosz P. Management of chronic kidney disease: the current novel and forgotten therapies. J Clin Transl Endocrinol 2024; 36: 100354.
3. Mansouri E, Assarehzadegan MA, Nejad-Dehbashi F, Kooti W. Effects of pravastatin in adriamycin-induced nephropathy in rats. Iran J Pharm Res 2018; 17: 1413-1419.
4. Jacevic V, Dragojevic-Simic V, Tatomirovic Z, Dobric S, Bokonjic D, Kovacevic A, *et al.* The efficacy of amifostine against multiple-dose doxorubicin-induced toxicity in rats. Int J Mol Sci 2018; 19: 2370.
5. Liu L, Zhao YF, Han WH, Chen T, Hou GX, Tong XZ. Protective effect of antioxidant on renal damage caused by doxorubicin chemotherapy in mice with hepatic cancer. Asian Pac J Trop Med 2016; 9: 1101-1104.
6. Jing L, Li L, Zhao J, Zhao J, Sun Z, Peng S. Zinc-induced metallothionein overexpression prevents doxorubicin toxicity in cardiomyocytes by regulating the peroxiredoxins. Xenobiotica 2016; 46: 715-725.
7. Kumral A, Giris M, Soluk-Tekkesin M, Olgac V, Dogru-Abbasoglu S, Turkoglu U, *et al.* Effect of olive leaf extract treatment on doxorubicin-induced cardiac, hepatic and renal toxicity in rats. Pathophysiology 2015; 22: 117-123.
8. Fujii J, Homma T, Osaki T. Superoxide radicals in the execution of cell death. Antioxidants (Basel) 2022; 11: 501.
9. Szponar J, Ciechanski E, Ciechanska M, Dudka J, Mandziuk S. Evolution of theories on doxorubicin-induced late cardiotoxicity: role of topoisomerase. Int J Mol Sci 2024; 25: 13567.
10. Akyol S, Ugurcu V, Altuntas A, Hasgul R, Cakmak O, Akyol O. Caffeic acid phenethyl ester as a protective agent against nephrotoxicity and/or oxidative kidney damage: A detailed systematic review. Sci World J 2014; 2014: 561971.
11. Soltani Hekmat A, Chenari A, Alipanah H, Javanmardi K. Protective effect of alamandine on doxorubicin-induced nephrotoxicity in rats. BMC Pharmacol Toxicol 2021; 22: 31.
12. Elsherbiny NM, El-Sherbiny M. Thymoquinone attenuates doxorubicin-induced nephrotoxicity in rats: Role of Nrf2 and NOX4. Chem Biol Interact 2014; 223: 102-108.
13. Ghosh J, Das J, Manna P, Sil PC. The protective role of arjunolic acid against doxorubicin-induced intracellular ROS-dependent JNK-p38 and p53-mediated cardiac apoptosis. Biomaterials 2011; 32: 4857-4866.
14. Mohamed RH, Karam RA, Amer MG. Epicatechin attenuates doxorubicin-induced brain toxicity: critical role of TNF-α, iNOS and NF-κB. Brain Res Bull 2011; 86: 22-28.
15. Alotiby A. Immunology of stress: a review article. J Clin Med 2024; 13: 6394.
16. Nikbakht J, Hemmati AA, Arzi A, Mansouri MT, Rezaie A, Ghafourian M. Protective effect of gallic acid against bleomycin-induced pulmonary fibrosis in rats. Pharmacol Rep 2015; 67: 1061-1067.
17. Azman PD, Yildirim S, Sengul E, Warda M, Tekin S, Aykurt F, *et al.* Protective effects of naringin against oxidative stress, inflammation, apoptosis and DNA damage in rats with doxorubicin-induced hepatotoxicity. Asian Pac J Trop Biomed 2025; 15: 285-295.
18. Kuzu M, Yildirim S, Kandemir FM, Kucukler S, Caglayan C, Turk E, *et al.* Protective effect of morin on doxorubicin-induced hepatorenal toxicity in rats. Chem Biol Interact 2019; 308: 89-100.
19. Benzer F, Kandemir FM, Kucukler S, Comakli S, Caglayan C. Chemoprotective effects of curcumin on doxorubicin-induced nephrotoxicity in Wistar rats by modulating inflammatory cytokines, apoptosis, oxidative stress and oxidative DNA damage. Arch Physiol Biochem 2018; 124: 448-457.
20. Moradi A, Abolfathi M, Javadian M, Heidarian E, Roshanmehr H, Khaledi M, *et al.* Gallic acid exerts nephroprotective, anti-oxidative stress and anti-inflammatory effects against diclofenac-induced renal injury in male rats. Arch Med Res 2021; 52: 380-388.
21. Tekin S, Sengul E, Yildirim S, Aksu EH, Bolat I, Cinar B, *et al.* Molecular insights into the antioxidative and anti-inflammatory effects of p-coumaric acid against bisphenol A-induced testicular injury: molecular docking and in silico studies. Reprod Toxicol 2024; 125: 108579.
22. Cicek B, Genc S, Yeni Y, Kuzucu M, Cetin A, Yildirim S, *et al.* Artichoke (Cynara scolymus) methanolic leaf extract alleviates diethylnitrosamine-induced toxicity in BALB/c mouse brain: involvement of oxidative stress and apoptotically related klotho/PPARγ signaling. J Pers Med 2022; 12: 2012.
23. Sulukan E, Baran A, Senol O, Kankaynar M, Yildirim S, Bolat I, *et al.* Global warming and glyphosate toxicity (I): Adult zebrafish modelling with behavioural, immunohistochemical and metabolomic approaches. Sci Total Environ 2023; 858: 160086.
24. Mohamadi Farsani F, Ganjalikhany MR, Dehbashi M, Naeini MM, Vallian S. Structural basis of DNA topoisomerase II-α inhibition: a computational analysis of interactions between Top2-α and its inhibitors. Med Chem Res 2016; 25: 1250-1259.
25. Wendorff TJ, Schmidt BH, Heslop P, Austin CA, Berger JM. The structure of DNA-bound human topoisomerase II alpha: conformational mechanisms for coordinating inter-subunit interactions with DNA cleavage. J Mol Biol 2012; 424: 109-124.
26. Kandemir FM, Kucukler S, Eldutar E, Caglayan C, Gulcin I. Chrysin protects rat kidney from paracetamol-induced oxidative stress, inflammation, apoptosis and autophagy: A multi-biomarker approach. Sci Pharm 2017; 85: 4.
27. Ikewuchi CC, Ifeanacho MO, Ikewuchi JC. Moderation of doxorubicin-induced nephrotoxicity in Wistar rats by aqueous leaf extracts of Chromolaena odorata and Tridax procumbens. Porto Biomed J 2021; 6: e129.
28. Xiang C, Yan Y, Zhang D. Alleviation of doxorubicin-induced nephrotoxicity by fasudil *in vivo* and *in vitro*. J Pharmacol Sci 2021; 145: 6-15.
29. Molski M. Theoretical study on the radical scavenging activity of gallic acid. Heliyon 2023; 9: e12806.
30. Nouri A, Heibati F, Heidarian E. Gallic acid exerts anti-inflammatory, anti-oxidative stress and nephroprotective effects against paraquat-induced renal injury in male rats. Naunyn Schmiedebergs Arch Pharmacol 2021; 394: 1-9.
31. Sharifi-Rigi A, Heidarian E. Therapeutic potential of *Origanum vulgare* leaf hydroethanolic extract against renal oxidative stress and nephrotoxicity induced by paraquat in rats. Avicenna J Phytomed 2019; 9: 563-573.
32. Kaymak E, Ozturk E, Akin AT, Karabulut D, Yakan B. Thymoquinone alleviates doxorubicin-induced acute kidney injury by decreasing endoplasmic reticulum stress, inflammation and apoptosis. Biotech Histochem 2022; 97: 622-634.
33. Khan TH, Ganaie MA, Alharthy KM, Madkhali H, Jan BL, Sheikh IA. Naringenin prevents doxorubicin-induced toxicity in kidney tissues by regulating oxidative and inflammatory insult in Wistar rats. Arch Physiol Biochem 2020; 126: 300-307.
34. Yufang W, Mingfang L, Nan H, Tingting W. Quercetin-targeted AKT1 regulates the Raf/MEK/ERK signaling pathway to protect against doxorubicin-induced nephropathy in mice. Tissue Cell 2023; 85: 102229.
35. Morsy MA, Ibrahim SA, Amin EF, Kamel MY, Rifaai RA, Hassan MK. Sildenafil ameliorates gentamicin-induced nephrotoxicity in rats: role of iNOS and eNOS. J Toxicol 2014; 2014: 489382.
36. Kang N, Lee JH, Lee W, Ko JY, Kim EA, Kim JS, *et al.* Gallic acid isolated from *Spirogyra* sp. improves cardiovascular disease through vasorelaxant and antihypertensive effects. Environ Toxicol Pharmacol 2015; 39: 764-772.
37. Abd El-Aziz TA, Mohamed RH, Pasha HF, Abdel-Aziz HR. Catechin protects against oxidative stress and inflammatory-mediated cardiotoxicity in adriamycin-treated rats. Clin Exp Med 2012; 12: 233-240.
38. Gandhi J, Khera L, Gaur N, Paul C, Kaul R. Role of modulator of inflammation cyclooxygenase-2 in gammaherpesvirus-mediated

tumorigenesis. Front Microbiol 2017; 8: 538.
39. Gao J, Gu Z. The role of peroxisome proliferator-activated receptors in kidney diseases. Front Pharmacol 2022; 13: 832732.
40. Masenga SK, Desta S, Hatcher M, Kirabo A, Lee DL. How PPAR-α mediated inflammation may affect the pathophysiology of chronic kidney disease. Curr Res Physiol 2025; 8: 100133.
41. Chen Z, Yuan P, Sun X, Tang K, Liu H, Han S, *et al*. Pioglitazone decreased renal calcium oxalate crystal formation by suppressing M1 macrophage polarization via the PPARγ–miR-23 axis. Am J Physiol Renal Physiol 2019; 317: F137-F151.
42. Singh JP, Singh AP, Bhatti R. Explicit role of peroxisome proliferator-activated receptor gamma in gallic acid-mediated protection against ischemia-reperfusion-induced acute kidney injury in rats. J Surg Res 2014; 187: 631-639.
43. Zhao X, Zhang L, Wu N, Liu Y, Xie J, Su L, *et al*. Gallic acid acts as an anti-inflammatory agent via PPARγ-mediated immunomodulation and antioxidation in fish gut-liver axis. Aquaculture 2024; 578: 740142.
44. Jia M, Han S, Li L, Fu Y, Zhou D. Interferon-stimulated genes: Novel targets in renal pathogenesis. Kidney Dis (Basel) 2025; 11: 390-401.
45. Tsiogkas SG, Apostolopoulou K, Mavropoulos A, Grammatikopoulou MG, Dardiotis E, Zafiriou E, *et al*. Gallic acid diminishes pro-inflammatory interferon-gamma- and interleukin-17-producing subpopulations *in vitro* in patients with psoriasis. Immunol Res 2023; 71: 475-487.
46. Eldutar E, Kandemir FM, Kucukler S, Caglayan C. Restorative effects of chrysin pretreatment on oxidant-antioxidant status, inflammatory cytokine production and apoptotic and autophagic markers in acute paracetamol-induced hepatotoxicity in rats. J Biochem Mol Toxicol 2017; 31: e21960.
47. Hassan MH, Ghobara M, Abd-Allah GM. Modulatory effects of meloxicam against doxorubicin-induced nephrotoxicity in mice. J Biochem Mol Toxicol 2014; 28: 337-346.
48. Mohamed EK, Hafez DM. Gallic acid and metformin co-administration reduce oxidative stress, apoptosis and inflammation via Fas/caspase-3 and NF-κB signaling pathways in thioacetamide-induced acute hepatic encephalopathy in rats. BMC Complement Med Ther 2023; 23: 265.
49. Zhou L, Zhou M, Tan H, Xiao M. Cypermethrin-induced cortical neuron apoptosis via the Nrf2/ARE signaling pathway. Pestic Biochem Physiol 2020; 165: 104547.
50. Loboda A, Damulewicz M, Pyza E, Jozkowicz A, Dulak J. Role of Nrf2/HO-1 system in development, oxidative stress response and diseases: an evolutionarily conserved mechanism. Cell Mol Life Sci 2016; 73: 3221-3247.
51. Li YC, Hao JC, Shang B, Zhao C, Wang LJ, Yang KL, *et al*. Neuroprotective effects of aucubin on hydrogen peroxide-induced toxicity in human neuroblastoma SH-SY5Y cells via the Nrf2/HO-1 pathway. Phytomedicine 2021; 87: 153577.
52. Schmidlin CJ, Dodson MB, Madhavan L, Zhang DD. Redox regulation by NRF2 in aging and disease. Free Radic Biol Med 2019; 134: 702-707.
53. de Oliveira MR, de Bittencourt Brasil F, Furstenau CR. Sulforaphane promotes mitochondrial protection in SH-SY5Y cells exposed to hydrogen peroxide by an Nrf2-dependent mechanism. Mol Neurobiol 2018; 55: 4777-4787.
54. Bao S, Lin J, Xie M, Wang C, Nie X. Simvastatin affects Nrf2/MAPK signaling pathway and hepatic histological structure changes in Gambusia affinis. Chemosphere 2021; 269: 128725.
55. Mohmmed Hegab AM, Hassanin SO, Mekky RH, Abuzahrah SS, Hamza AA, Talaat IM, *et al*. Withania somnifera ameliorates doxorubicin-induced nephrotoxicity and potentiates its therapeutic efficacy targeting SIRT1/Nrf2, oxidative stress, inflammation and apoptosis. Pharmaceuticals (Basel) 2025; 18: 248.
56. Lu C, Wei J, Gao C, Sun M, Dong D, Mu Z. Molecular signaling pathways in doxorubicin-induced nephrotoxicity and potential therapeutic agents. Int Immunopharmacol 2025; 144: 113373.
57. Khalaf MM, Hassanein EHM, Qebesy HS, Ahmed AA, Mahmoud HM. Granisetron ameliorates doxorubicin-evoked nephrotoxicity via modulation of Nrf2 and TLR4/p38 MAPK/NLRP3 signaling in rats. Tissue Cell 2025; 93: 102744.